

The Functional Width of the Dentino-Enamel Junction Determined by AFM-Based Nanoscratching

Stefan Habelitz,¹ Sally J. Marshall, Grayson W. Marshall Jr., and Mehdi Balooch*

Department of Preventive and Restorative Dental Sciences, University of California, San Francisco, San Francisco, California 94143; and *Department of Chemistry and Materials Science, Lawrence Livermore National Laboratory, Livermore, California 94550

Received June 26, 2001, and in revised form August 8, 2001; published online October 26, 2001

The dentino-enamel junction (DEJ) constitutes a structurally unique interphase uniting two mineralized tissues with very different matrix composition and physical properties. Its excellent biomechanical properties have drawn interest as a biomimetic model for joining dissimilar materials. In order to characterize the functional width of the DEJ, nanoscratching experiments were performed on human third molars. Friction coefficients of enamel, of dentin, and at the DEJ were obtained with a nanoscratch tester attached to an atomic force microscope (AFM). Normal loads in the range of 50 to 600 μN were applied to a spherical diamond indenter ($r = 10 \mu\text{m}$), which was driven 10 μm across the sample surface, recording the lateral force. Imaging with an AFM facilitated exact positioning of the scratches. The friction coefficient of intertubular dentin was 0.31 ± 0.05 , significantly above the coefficient of enamel of 0.14 ± 0.02 . The increased friction of dentin is attributed to the higher content of organic phases. Scratches performed across the interphase between enamel and dentin showed a sharp monotonic change in the friction coefficient. The average width of the slope between the friction coefficients of dentin and enamel was $2.0 \pm 1.1 \mu\text{m}$ and is assumed to represent the functional width of the dentino-enamel junction. The effect of the scalloped structure of the DEJ on its functional width as determined by mechanical testing is discussed. © 2001 Elsevier Science

Key Words: atomic force microscopy; nanoindentation; nanoscratch testing; friction coefficient; dentino-enamel junction; tooth.

¹ To whom correspondence should be addressed at Department of Preventive and Restorative Dental Sciences, University of California, San Francisco, 707 Parnassus Avenue, D-2250, San Francisco, CA 94143-0758. Fax: (415) 476-0858. E-mail: shabeli@itsa.ucsf.edu.

INTRODUCTION

The dentino-enamel junction (DEJ) is a natural junction that unites two mechanically dissimilar calcified tissues in the tooth: the hard and brittle enamel and the softer and tougher dentin. The DEJ is considered as an interphase, which is defined as a region of distinct or functionally graded properties between two or more phases (Fong *et al.*, 2000; Marshall *et al.*, 2001; Urabe *et al.*, 2000; White *et al.*, 2000). As such it would be distinguished from an interface, which refers to the presence of a sharp two-dimensional boundary between two phases (Hodzic *et al.*, 2000b). The DEJ appears to play a key role in preventing the transmission of cracks through enamel and into dentin. As such, it may serve as a useful model for biomimetic formulations in which mechanically dissimilar biomaterials must be joined to restore form and function (Lin and Douglas, 1994; Urabe, 2000; Fong, 2000; Marshall *et al.*, 2001).

The structure of the DEJ is generally described as having 25- to 100- μm -diameter scallops with their convexities directed toward the dentin (Arsenault and Robinson, 1989; Hayashi, 1992; Lustmann, 1978; Rywkind, 1931; Scott and Symons, 1971; Sela *et al.*, 1975; Ten Cate, 1994; Whittaker, 1978). These scallops contain microscallops and finer structures. Besides the unique structure, the presence of a smooth gradient of mechanical properties at the junction is thought to contribute to the interfacial bonding between enamel and dentin and is considered an important toughening mechanism that reduces stress concentrations. In order to obtain this gradation of properties a precise control of protein expression and biomineralization at the junction has been suggested (Fong *et al.*, 2000; White *et al.*, 2000).

Measurements of the functional or mechanical width of an interphase require either a number of independent measurements of properties spanning

the interphase or a technique that provides continuous data collection across the interphase. Indentation techniques have been used to obtain mechanical properties at discrete points across the DEJ. From the gradient in hardness or elastic modulus, functional widths of the DEJ have been estimated using either micro- or nanoindentations. Several authors showed that mechanical properties displayed a monotonic transition from enamel to dentin when indentations spanned the DEJ (Fong *et al.*, 2000; Marshall *et al.*, 2001; Urabe *et al.*, 2000; Wang and Weiner, 1998; White *et al.*, 2000). However, large variations in the proposed width of the DEJ have been reported for different techniques. Using microhardness, a width of 100 to 200 μm was suggested (Wang and Weiner, 1998; White *et al.*, 2000), while nanoindentation measurements revealed a width of 12 to 20 μm (Fong *et al.*, 2000; Marshall *et al.*, 2001; Urabe *et al.*, 2000). However, using an indentation technique to quantify spatial variations of an interface is difficult. Sufficient spacing between indentations (about four times the indentation size) must be maintained to ensure appropriate properties determination. Furthermore, the three-dimensional scalloped structure of the DEJ and its multilevel substructure should be taken into consideration when mechanical properties are obtained from cross sections through this junction.

The observations of a broad transitional zone between enamel and dentin are in contrast with data acquired by high-resolution imaging at this junction. Several authors indicated that if at all, only a narrow interfacial zone between the mantle dentin and enamel is present (Bodier-Houille *et al.*, 2000; Hayashi, 1992; Lin *et al.*, 1993). Studies using transmission electron microscopy at the DEJ showed frequent bridging of collagen fibrils from the dentin into the enamel. The fibrils, however, did not reach further into the enamel than a few hundred nanometers. The junction was more typified by an abrupt structural demarcation, comparable to the presence of a plain interface, between dentin and enamel. This demarcation line, however, was very irregular, showing deep interpenetrations of the two phases due to the scalloped architecture of the junction.

In this study, the concept of continuously monitoring properties along a line was applied to the DEJ using a nanoscratching technique that facilitates the continuous recording of the friction coefficient. In the field of protective and wear-resistant coatings, the scratch test is a common tool for characterizing the mechanical resistance of the coating-substrate interface (Benjamin and Weaver, 1960; Li and Bhushan, 1999; Steinmann *et al.*, 1987). As such, the adhesion forces and scratch hardness of paints are measured by straining the coating with

an increasing load on the stylus until cracking occurs.

The development of nanoindentation techniques enabled measurements of mechanical properties of layers and structural entities on the nanometer scale. Thus, site-specific information, e.g., hardness and elastic modulus, of microfeatures in biological tissues and synthetic materials can be obtained (Habelitz *et al.*, 2001; Kinney *et al.*, 1996; Rho *et al.*, 1997; Zysset *et al.*, 1999). Recent progress in nanotest methods facilitated lateral movement of a nanoindenter while simultaneously recording the lateral force. Nanosized scratch tests are widely used to characterize thin films on semiconductor substrates with thicknesses as low as a few nanometers (Kriese *et al.*, 1998; Venkataraman, 1996).

Nanoscratch testing recently has been used to measure friction of material surfaces (Wang *et al.*, 2000). In the absence of plastic deformation, the friction coefficient μ can be determined as the quotient of lateral to normal force, between stylus and sample surface. Friction forces, however, depend not only on the attractive forces between sample surface and sliding stylus, but also on several extrinsic materials properties. For example, surface roughness and stylus geometry are difficult to control and can tremendously alter the frictional behavior (Bulduum *et al.*, 1998; Steinmann, 1987). Thus, results must be interpreted as qualitative or semiquantitative. However, using this technique to measure frictional forces would provide data sets that enable the quantification of the two-dimensional size of material phases with significant differences in their friction properties. The application of lateral force microscopy, for example, is based on the ability to detect differences in the friction properties on the nanometer scale in order to acquire images of sample surfaces (Gibson *et al.*, 1997).

For the present study the approach of Hodzic *et al.* (2000a,b), who performed the scratches of a few nanometers in diameter across a glass-polymer interphase and determined the functional width of the interphase, is employed. Here, nanoscratches are conducted on enamel, on dentin, and across the DEJ of human teeth, and their friction coefficient profiles are recorded in order to determine the functional width of the DEJ.

MATERIALS AND METHODS

Human third molars with documented history were extracted according to protocols approved by the UCSF Committee on Human Research. Teeth were sterilized by gamma radiation and stored (less than 4 months) in deionized water at 4°C until prepared (White *et al.*, 1994). Sagittal midcoronal sections (thickness of 2 mm) were prepared by polishing through a series of SiO₂ papers and with a diamond paste to 0.25 μm . Ultrasonic treatments in water for 10 s were used to clean the surface. Specimens

were glued with cyanoacrylate to a metal disk for study in the atomic force microscope (AFM).

Nanoindentations and nanoscratches were performed using an AFM (Nanoscope III, Digital Instruments, Santa Barbara, CA) with the standard head replaced by a 2D-Tribo-Scanner (Hysitron Inc., Minneapolis, MN), which consists of two transducers. One transducer controls displacement and force in the vertical axis, which is the common assembly for nanoindentation experiments (Oliver and Pharr, 1992). The second transducer is attached perpendicular to the vertical transducer and records horizontal displacement and lateral forces applied to move the indenter across the specimen's surface. Before a series of measurements, calibration of the lateral force transducer was performed in air for the entire scratch length of 10 μm . In a typical experiment, an adequate area was selected, e.g., intertubular dentin or DEJ, using the imaging capabilities of the AFM. Then constant normal loads (L_N) were applied, pressing the indenter onto the sample surface, trying to avoid plastic deformation in order to obtain pure frictional behavior. However, depending on the load and the hardness of the substrate, the indenter can slightly penetrate into the material. Subsequently, the indenter was driven horizontally across the sample surface while the normal force was maintained. Lateral (L_L) and normal forces (L_N), as well as normal and lateral displacements were recorded during the scratch test. Lateral or frictional forces opposing the sliding movement of the indenter and the substrate were attributed to three components: adhesion forces, elastic deformation of surface asperities, and plowing forces or plastic deformation. The last forces should be minimized in order to ensure pure frictional behavior (Suh and Sin, 1981). Hence a relatively blunted tip, a spherical diamond tip with a tip radius of 10 μm (Hysitron Inc., MN), and low loads of 50, 100, 200, 300, or 600 μN were applied. A scratch length of 10 μm and a scratch rate of 333 nm/s were chosen for the experiment. The friction coefficients (μ) were monitored with 1000 data points over the whole length of the scratch and were calculated from the equation $\mu = L_L/L_N$.

Friction coefficients of the intertubular dentin within the mantle dentin and enamel at areas close to the DEJ (distance <200 μm) were determined. A minimum of 3 scratches at each load on dentin and enamel of each tooth were conducted. Subsequently, scratches across the DEJ were performed in both directions, from dentin toward enamel and vice versa. The functional width of the DEJ was determined by measuring the width of the slope between friction coefficients attributed to dentin and enamel. The average functional width of the DEJ was obtained from 48 scratches at loads between 100 and 600 μN on all three teeth studied.

RESULTS

Figure 1 shows AFM images of nanoscratches conducted on human dentin (Fig. 1a), on enamel (Fig. 1b), and across the DEJ (Fig. 1c) at loads as indicated for each scratch. Nanoscratches were visible only if scratch tests were performed at loads of at least 200 or 100 μN on dentin and enamel, respectively. The use of AFM facilitated the exact placement of scratches on intertubular dentin, avoiding scratching across peritubular dentin and tubules, which have different friction characteristics. Scratches on enamel crossed at least one entire rod and were performed without respect to the rod orientation. AFM images of the DEJ revealed a surface step between dentin and enamel as shown in Fig. 1c. Due to differences in elastic modulus, the softer

dentin deforms more under the pressure applied for polishing and the surface level of dentin appears to be about 100 to 250 nm below the enamel level after polishing. Scratches at the DEJ were conducted crossing the junction perpendicularly. The scratches were more profound on the dentin side. At a load of 300 μN the scratch depth was approximately 25 ± 5 nm, as determined from the AFM images. Scratches on the enamel side were shallower and thus more difficult to image because resolution decreased at the DEJ due to the higher surface roughness and increased z range (see Fig. 1c).

Figure 2 shows a characteristic course of lateral and normal force versus displacement obtained during scratching across enamel. Data points were recorded every 10 nm for the whole scratch length of 10 μm . The normal load, which was set to 300 μN , varied between 275 and 320 μN , which was attributed to adjustments to surface irregularities and specimen tilt. The lateral force in this experiment varied between 43 and 53 μN . Background noise of the lateral force increased significantly with decreasing loads. Friction coefficients were obtained for the whole scratch length from the quotient of lateral to normal force. Characteristic friction coefficient courses for dentin (a), enamel (c), and the DEJ (b) are shown in Fig. 3. Courses of friction coefficients of dentin (curve a) had a relatively high background noise compared to enamel (curve c), which is attributed to the increased surface roughness of dentin. Curve b of Fig. 3 shows an abrupt transition in friction forces when scratches cross the DEJ. Average friction coefficients of 0.31 ± 0.05 and 0.14 ± 0.02 for dentin and enamel, respectively, were calculated from all specimens studied and for the whole range of loads applied. Friction coefficients of enamel remained approximately constant for loads between 50 and 600 μN , as shown in Fig. 4. The friction coefficient curve of dentin showed a higher noise level, which is attributed to an increased surface roughness compared to enamel. The friction coefficient of dentin was about 0.3 for loads between 50 and 300 μN . At loads of 600 μN the friction coefficient dropped slightly to 0.25. High standard deviations at low loads are attributed to more background noise of the lateral force recording. Scratching from dentin toward enamel showed a continuous and sharp decrease in friction coefficients. Within a lateral displacement or scratch length of a few micrometers the friction coefficients decreased from the level of the intertubular dentin to a level slightly above the level of enamel. The lateral displacement, which is covered by the slope between the friction coefficients of dentin and enamel, was considered to be the functional width of the DEJ. Figure 5 illustrates how the width was

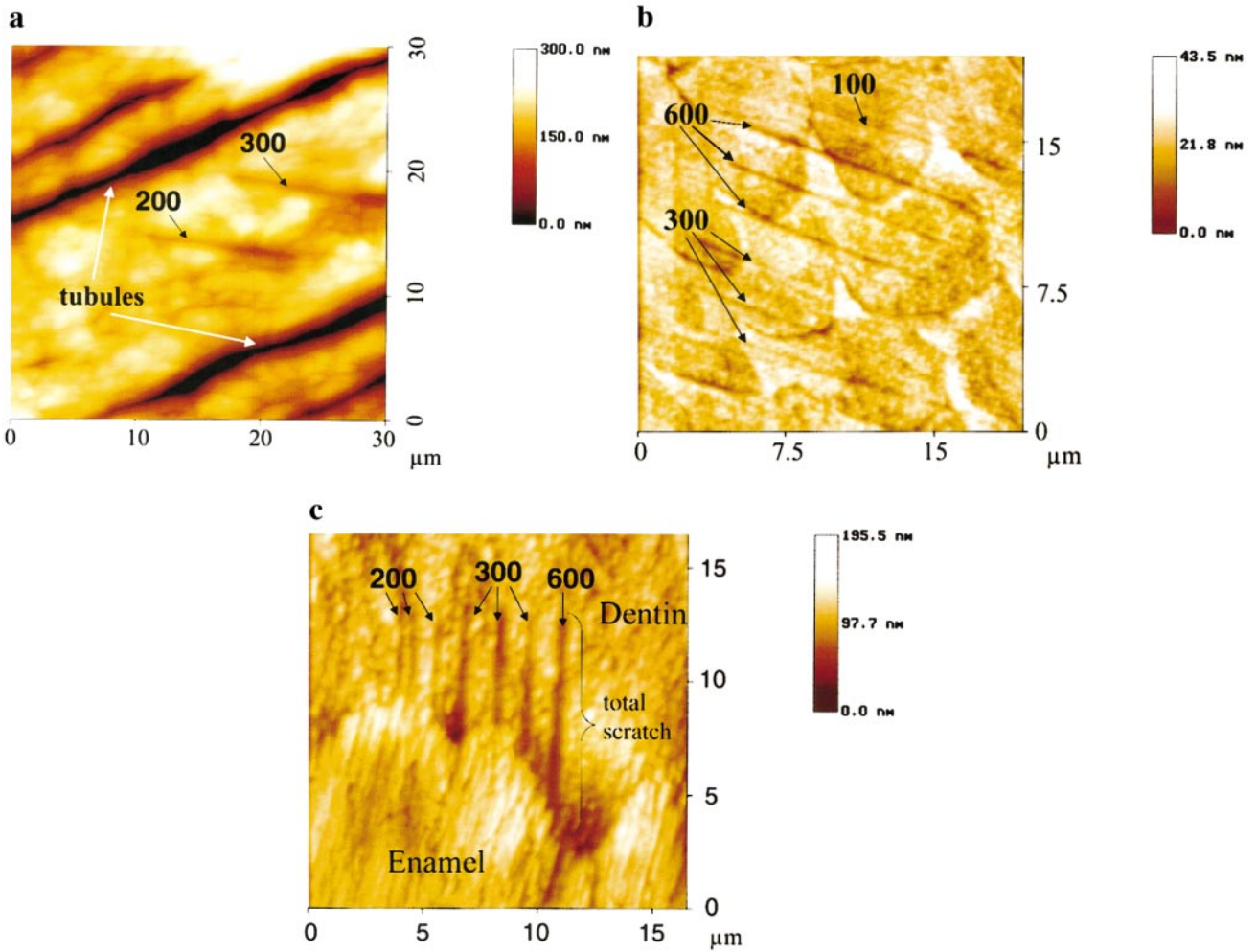


FIG. 1. AFM images of nanoscratches across (a) intertubular dentin, (b) enamel rods, and (c) dentino-enamel junction of human third molars. Numbers indicate the load applied in micronewtons. The color schemes show the z range of the images, with brighter colors indicating increased topographic height in a linear scale.

determined. Forty-eight scratches across the DEJ of three different teeth at loads between 100 and 600 μN were evaluated and resulted in an average width of $2.0 \pm 1.1 \mu\text{m}$. A slight increase in the functional width with normal force was observed. Average widths of 1.7, 1.8, 2.2, and 2.5 μm were determined at loads of 100, 200, 300, and 600 μN, respectively. However, the differences in width were not significant ($P > 0.05$, ANOVA). When scratching was conducted in the opposite direction, from enamel toward dentin, a similar friction coefficient profile was obtained. The friction coefficient increased from the level of the enamel to the level of the dentin within $1.6 \pm 0.7 \mu\text{m}$ and was not significantly different from results obtained from scratch tests performed in the other direction. The course of the friction coefficients at the DEJ often showed a mono-

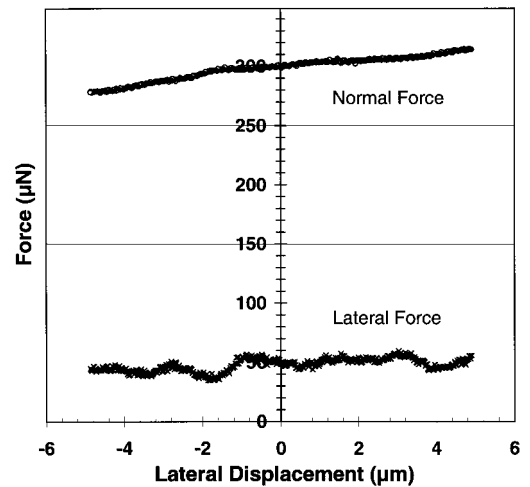


FIG. 2. Force–displacement courses for a scratch of 10 μm on enamel: Normal load was set to 300 μN and resulted in a lateral force of around 45 μN.

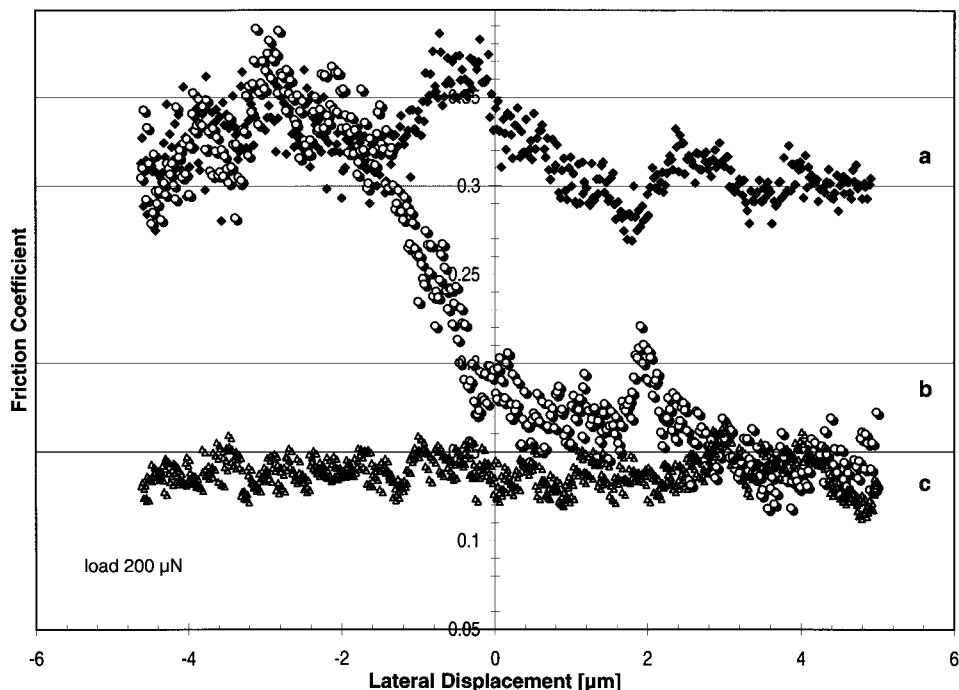


FIG. 3. Courses of friction coefficients versus lateral displacement: Nanoscratches were performed at 200- μ N normal force (a) on dentin, (b) across DEJ, and (c) on enamel.

tonic slope, but occasionally also revealed sudden shifts in the friction behavior, illustrated as humps in Fig. 5.

DISCUSSION

Nanoscratches conducted on enamel and intertubular dentin yielded friction coefficients of these tissues for the particular indenter used. The friction coefficient of dentin was significantly higher than

that of enamel, which can be attributed to the higher content of organic phases in intertubular dentin (~ 45 vol%) (Butler, 1998) compared to enamel (~ 12 vol%), which is also reflected in the lower hardness and elastic modulus of dentin (Habelitz *et al.*, 2001; Kinney *et al.*, 1996).

Using an AFM for exact positioning, scratch tests were performed crossing the DEJ. A very narrow transitional zone of friction properties between the dentin and enamel was revealed. The width of the gradient in friction coefficients at the DEJ was on the order of $2 \mu\text{m}$ and is assumed to be the functional width of the DEJ. This width is significantly lower than values obtained by nano- or microindentation techniques. As shown by Hodzic *et al.* (2000b) for glass-polymer interfaces, scratch tests can provide improved estimates of mechanical property changes at interphases. The advantage of nanoscratch testing versus nanoindentation lies in the continuous measurement of properties. Whereas nanoindentations placed along a line require spacing to avoid interaction of the plastic zone and the contact stress fields, nanoscratching allows continuous reading of the frictional properties along the line or scratch and thus improves the spatial resolution of the measurement.

Furthermore, deep penetration into the material was avoided by using a blunted indenter for scratch testing at low loads. Scratch depths between 10 and

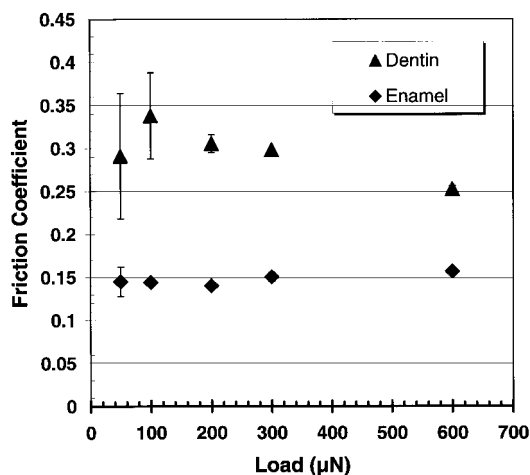


FIG. 4. Friction coefficients of enamel and dentin at different loads (error bars are standard deviations).

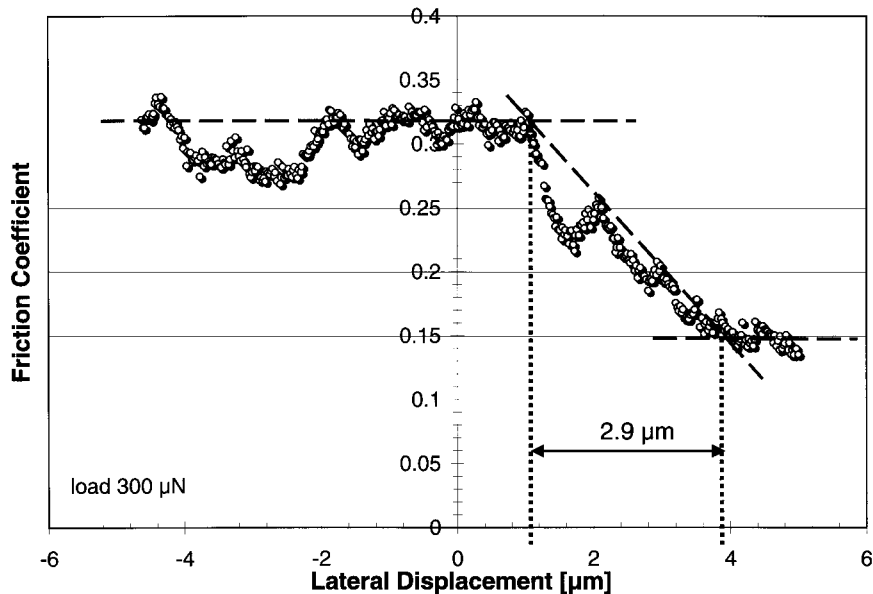


FIG. 5. Analysis of a course of friction coefficients obtained by scratching across the DEJ at a normal load of 300 μN . The width of the slope relates to the functional width of the DEJ.

40 nm were measured on dentin at loads between 200 and 600 μN . Thus, the interaction of the tip with the material is mostly reduced to the surface. In contrast, sharp indenters (e.g., Vickers, Berkovich, or cube corner) cause larger and deeper indentations, as illustrated by a comparison of indentation studies found in the literature and are summarized in Table I. In particular, the use of a microindenter, although applied at relatively low loads, increases the indentation size and depth by several times. As shown by Hodzic *et al.* (2000b) reliable values of the width of an interphase are facilitated only if the size of the indentation is significantly smaller than the size of the interphase. Since the interfacial zone of distinct mechanical properties between the enamel and dentin is only a few micrometers, large indentations would not be valuable. Thus, microindenta-

tions may overestimate the actual size of the junction due to averaging the dentin and enamel hardness within individual indentations close to the DEJ (White *et al.*, 2000). Indentations at the submicrometer level have a better spatial resolution. However, the indentations need to be spaced to avoid interactions, which then decrease the spatial information of the measurement.

The DEJ shows several levels of scallop-like structures, which in cross sections appear as concavities pointed toward the enamel (Whittaker, 1978). As such, it is a highly irregular, nonplanar junction. Using indentation methods on such a three-dimensional feature means that indentations may sample varying mixtures of the phases on either side of the junction. The deeper the indentation at the DEJ, the more likely is an interaction with an underlying

TABLE I
Comparison of Indentation Characteristics from Studies Conducted across the DEJ

Type of indenter	Load	Indentation depth on human dentin	Indentation size at surface	Step size	Width DEJ
Vickers microindentation ^a	147 mN	3.4 μm	17 μm	50 μm	27–100 μm
Berkovich nanoindentation ^b	1 mN	100 nm	850 nm	>2 μm	15–25 μm
Cube corner nanoindentation ^c	500 μN	300 nm	800 nm	1–2 μm	10–13 μm
Spherical nanoscratchtester ^d	300 μN	25 nm	1.4 μm	0 μm	1–3 μm

Note. Dimensions refer to indentations on the dentin side.

^a White *et al.* (2000).

^b Fong *et al.* (2000).

^c Marshall *et al.* (2001).

^d This study.

phase different from the DEJ, e.g., dentin or enamel. Figure 6 is a schematic drawing of nanoindentations at the junction, where the DEJ is considered as a plain, but irregular interface. In both cases shown, the indentation penetrates two phases, enamel and dentin, resulting in a combination of mechanical properties, which are distinct from the properties of the single phases. Avoiding deep penetrations should therefore allow a more accurate measurement of the functional width.

This consideration is supported by the trend shown in the literature that a decreasing indentation depth results in a decreased width of the DEJ (Table I). Hence, an extrapolation of the resulting widths obtained from measurements at various loads might be suitable to narrow down the size of the DEJ. The width obtained at loads $L_N = 0$ N would theoretically correspond to the width measured by an infinitely low load or an infinitely small tip. We applied this approach to our results and Fig. 7 shows a plot of load versus width of the DEJ. A decrease of the width was observed with decreasing loads. According to a regression analysis, the width of the DEJ at $L_N = 0$ would be about $1.6 \mu\text{m}$ and is as such within the range determined by nanoscratching. This approach, however, seems critical since the widths obtained at loads between 100 and $600 \mu\text{N}$ were not significantly different ($P > 0.05$).

Using nanoscratch testing an approximately monotonic linear transition of the properties across the junction was observed, which is in good agreement with results from nanoindentation experiments (Fong *et al.*, 2000; Marshall *et al.*, 2001; Urabe *et al.*, 2000). However, to what extent this observation depicts the true mechanical behavior remains questionable. A monotonic slope of property

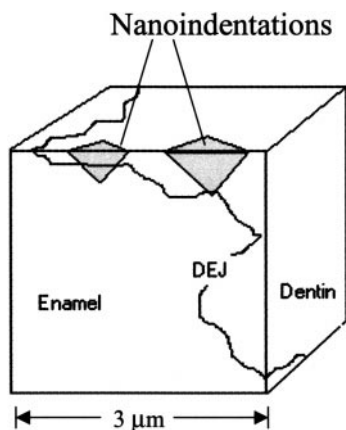


FIG. 6. Schematic drawing of nanoindentations at the DEJ. Due to the three-dimensional structure of the DEJ, nanoindentations can penetrate dentin and enamel, resulting in an average value of mechanical properties.

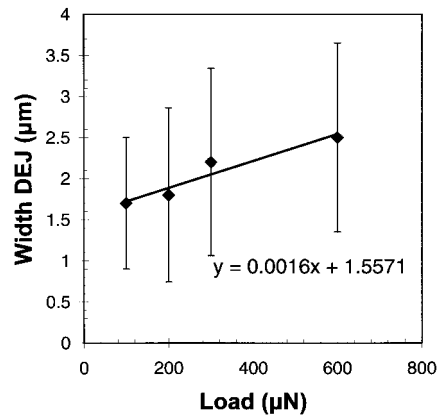


FIG. 7. The average functional width of the DEJ at different loads applied: Width decreases with load. Extrapolation yields a width of $1.6 \mu\text{m}$ at a load of $0 \mu\text{N}$ (error bars are standard deviations).

values at a junction can, on one hand, represent its true behavior. On the other hand, it is likely to be the result of a superimposition and averaging of properties of the single phases (Hodzic *et al.*, 2000b). With a minimum contact area of the spherical indenter with the specimen surface of about $1 \mu\text{m}$ in diameter, nanoscratch testing would not be capable of measuring the actual dimension of the DEJ if it is formed of an interphase below $1 \mu\text{m}$ in size or if it consists of a simple interface. Applying the scratch test to quantify the size of highly irregular interfaces, however, does not eliminate the influence of the angle in which the interface is crossed on the width of this interface. In this study we attempted to maintain the direction of the nanoscratches perpendicular to the orientation of the DEJ. However, due to its scalloped architecture, scratches sometimes followed the curved interfacial line tangentially (Fig. 1c) before crossing. This could increase the size of the transition zone in the lateral force profiles and is assumed to be a reason for the relatively high standard deviations of the average width of the DEJ ($2.0 \pm 1.1 \mu\text{m}$).

Hence, in order to better understand property phenomena at the DEJ we are currently studying the three-dimensional structure of this junction. Simulations of the DEJ interpenetrating architecture relating structure to properties might further elucidate the real width of the DEJ. Regarding biomimetic modeling of the DEJ, emphasis on the interfacial design concerning its microstructural organization and roughness is encouraged in order to improve joining of materials with different mechanical properties.

CONCLUSIONS

This study introduces nanoscratch testing as a useful method to determine functional dimensions of interfaces in biological hard tissues. By continuous recording of the frictional forces along a line crossing the junction between enamel and dentin, a functional width of the dentino-enamel junction of human third molars of approximately 2 μm was determined.

The authors appreciate the helpful suggestions for data evaluation by Dr. Brian R. Lawn, National Institute of Standards and Technology (Gaithersburg, MD) and the financial support by NIH/NIDCR Grant DE13029.

REFERENCES

- Arsenault, A. L., and Robinson, B. W. (1989) The dentino-enamel junction: A structural and microanalytical study of early mineralization. *Calcif. Tissue Int.* **45**, 111–121.
- Benjamin, P., and Weaver, C. (1960) Adhesion of metal films to glass. *Proc. R. Soc. London A* **254**, 177–183.
- Bodier-Houille, P., Steuer, P., Meyer, J. M., Bigeard, L., and Cuisinier, F. J. (2000) High-resolution electron-microscopic study of the relationship between human enamel and dentin crystals at the dentinoenamel junction. *Cell Tissue Res.* **301**, 389–395.
- Buldum, A., Ciraci, S., and Batra, I. P. (1998) Contact, nanoindentation, and sliding friction. *Phys. Rev. B Condens. Matter* **57**, 2468–2476.
- Butler, W. T. (1998) Dentin matrix proteins. *Eur. J. Oral Sci.* **106**(Suppl.1), 204–210.
- Fong, H., Sarikaya, M., White, S. N., and Snead, M. L. (2000) Nano-mechanical properties profiles across dentin–enamel junction of human incisor teeth. *Mater. Sci. Eng.* **C7**, 119–128.
- Gibson, C. T., Watson, G. S., and Myhra, S. (1997) Lateral force microscopy—A quantitative approach. *Wear* **213**, 72–79.
- Habelitz, S., Marshall, S. J., Marshall, G. W., and Balooch, M. (2001) Mechanical properties of human dental enamel on the nanometer scale. *Arch. Oral Biol.* **46**, 173–183.
- Hayashi, Y. (1992) High resolution electron microscopy in the dentino-enamel junction. *J. Electron Microsc.* **41**, 387–391.
- Hodzic, A., Kim, J. K., and Stachurski, Z. H. (2000a) The nanoscratch technique as a novel method for measurement of an interphase width. *J. Mater. Sci. Lett.* **19**, 1665–1667.
- Hodzic, A., Stachurski, Z. H., and Kim, J. K. (2000b) Nanoindentation of polymer–glass interfaces. I. Experimental and mechanical analysis. *Polymer* **41**, 6895–6905.
- Kinney, J. H., Balooch, M., Marshall, S. J., Marshall, G. W., Jr., and Weihs, T. P. (1996) Hardness and Young's modulus of human peritubular and intertubular dentine. *Arch. Oral Biol.* **41**, 9–13.
- Kriese, M. D., Boismier, D. A., Moody, N. R., and Gerberich, W. W. (1998) Nanomechanical fracture-testing of thin films. *Eng. Fract. Mech.* **61**, 1–20.
- Li, X., and Bhushan, B. (1999) Micro/nanomechanical and tribological characterization of ultrathin amorphous carbon coatings. *J. Mater. Res.* **14**, 2328–2337.
- Lin, C. P., and Douglas, W. H. (1994) Structure–property relations and crack resistance at the bovine dentin–enamel junction. *J. Dent. Res.* **73**, 1072–1078.
- Lin, C. P., Douglas, W. H., and Erlandsen, S. L. (1993) Scanning electron microscopy of type I collagen at the dentin–enamel junction of human teeth. *J. Histochem. Cytochem.* **41**, 381–388.
- Lustmann, J. (1978) Dentinoenamel junction area in primary teeth affected by Morquio's syndrome. *J. Dent. Res.* **57**, 475–479.
- Marshall, G. W., Balooch, M., Gallagher, R. R., Gansky, S. A., and Marshall, S. J. (2001) Mechanical properties of the dentinoenamel junction: AFM studies of nanohardness, elastic modulus, and fracture. *J. Biomed. Mater. Res.* **54**, 87–95.
- Oliver, W. C., and Pharr, G. M. (1992) An improved technique for determining hardness and elastic modulus using load and displacement sensing indentation experiments. *J. Mater. Res.* **7**, 1564–1583.
- Rho, J.-Y., Tsui, T. Y., and Pharr, G. M. (1997) Elastic properties of human cortical and trabecular lamellar bone measured by nanoindentation. *Biomaterials* **18**, 1325–1330.
- Rywkind, A. W. (1931) So-called scalloped appearance of the dentino-enamel junction. *J. Am. Dent. Assoc.* **18**, 1103–11010.
- Scott, J. H., and Symons, N. B. B. (1971) Introduction to Dental Anatomy, 6th ed. Livingstone, Edinburgh.
- Sela, J., Sela, M., Lustmann, J., and Ulmansky, M. (1975) Dentinoenamel junction area of a resorbing permanent incisor studied by means of scanning electron microscopy. *J. Dent. Res.* **54**, 110–113.
- Steinmann, P. A., Tardy, Y., and Hintermann, H. E. (1987) Adhesion testing by the scratch test method: The influence of intrinsic and extrinsic parameters on the critical load. *Thin Solid Films* **154**, 333–349.
- Suh, N. P., and Sin, H. C. (1981) The genesis of friction. *Wear* **69**, 91–114.
- Ten Cate, A. R. (1994) Oral Histology: Development, Structure, and Function, 4th ed. Mosby, St. Louis.
- Urabe, I., Nakajima, M., Sano, H., and Tagami, J. (2000) Physical properties of the dentin–enamel junction region. *Am. J. Dent.* **13**, 129–135.
- Venkataraman, S., Kohlstedt, D. L., Gerberich, W. W. (1996) Continuous microscratch measurements of the practical and true work of adhesion for metal/ceramic systems. *J. Mater. Res.* **11**, 3133–3145.
- Wang, J. G., Choi, B. W., Nieh, T. G., and Liu, C. T. (2000) Nano-scratch behavior of a bulk Zr–10Al–5Ti–17.9Cu–14.6Ni amorphous alloy. *J. Mater. Res.* **15**, 913–922.
- Wang, R. Z., and Weiner, S. (1998) Strain–structure relations in human teeth using Moiré fringes. *J. Biomech.* **31**, 135–141.
- White, J. M., Goodis, H. E., Marshall, S. J., and Marshall, G. W. (1994) Sterilization of teeth by gamma radiation. *J. Dent. Res.* **73**, 1560–1567.
- White, S. N., Paine, M. L., Luo, W., Sarikaya, M., Fong, H., Yu, Z. K., et al. (2000) The dentino-enamel junction is a broad transitional zone uniting dissimilar bioceramic composites. *J. Am. Ceram. Soc.* **83**, 238–240.
- Whittaker, D. K. (1978) The enamel–dentine junction of human and *Macaca irus* teeth: A light and electron microscopic study. *J. Anat.* **125**, 323–335.
- Zysset, P. K., Guo, X. E., Höffler, C. E., Moore, K. E., and Goldstein, S. A. (1999) Elastic modulus and hardness of cortical and trabecular bone lamellae measured by nanoindentation in the human femur. *J. Biomech.* **32**, 1005–1012.